IEEE Access
Multidisciplinary | Rapid Review | Open Access Journal

Date of publication xxxx 00, 0000, date of current version xxxx 00, 0000.

Digital Object Identifier 10.1109/ACCESS.2017.DOI

Mapping Functions Driven Robust Retinal Vessel Segmentation via Training Patches

HAIYING XIA[1], FRANK JIANG[1,2,*],
[1]College of Electronics Engineering, Guangxi Normal University, China
[2]Faculty of Engineering and IT, University of Technology Sydney, Australia

*Corresponding author: Frank Jiang (e-mail: Frank.Jiang@uts.edu.au).

This work was supported in part by the National Natural Science Foundation of China (No.61762014; 61762018)

ABSTRACT Vein occlusions and diabetic retinopathy are two of many retinal pathologies affecting the retina. Understanding robust vessel segmentation of fundus images is of vital importance of improving the diagnosis results of these diseases. For the first time, this paper proposes a new approach of computing the minimum distance for each test patch via the distance comparison within the test patch and cluster centres. The numerous patches are calculated via the manual segmentations through K-means algorithm. We demonstrate the efficiency of learning the simple pattern from each cluster, meanwhile, the mapping function for each cluster is determined by the patches in training images and their corresponding manual segmentation patches. Two publicly recognized benchmark datasets DRIVE and STARE are used in our experimental validation. Experimental results show that our methodology achieves a modest performance for vessel segmentation on public datasets in comparison with the recent state-of-the-art methods.

INDEX TERMS fundus images,mapping functions, vessel segmentation

I. INTRODUCTION

DIABETIC retinopathy, one of retinal pathologies, is reported as the leading cause of blindness for the aged population worldwide, though other retinal pathologies include retinopathy of prematurity, retinoblastoma and vein occlusions are also reported in the literature as the supplementary causes. In this paper, we focus on providing the suitable approach for vein occlusions and diabetic retinopathy via the new segmentation method and the flowchart of our method is shown in Figure 1.

It is known that color fundus imaging assists in retinal disease diagnosis through portraying an image of the retina. However, the difficulty of this research is to find a suitable classifier to enable further analysis of the color fundus imaging by adjusting retinal vein segmentation to generate accurate blood vessel binary images [1]. It is argued that through comprehensive design of feature extraction, a new classifier can better classify color fundus images.

In particular, taken the fundus images as an example of retinal pathologies, the solutions for these images mainly suffer from low resolution and noise. While big vessels can be segmented accurately, tiny vessels remain a challenge as they cannot be distinguished from the noisy background. Machine learning techniques can help overcome the tiny vessel challenge in fundus images [2] [3] [4] [5] [6] [7]. Vessel pixels can be distinguished from other pixels using classifiers. However, this process is tedious, slow and inefficient due to several issues. First of all, due to the characteristics of the device, the fundus image is low contrast, which will lead to the degradation of the discriminator's discriminative power. Second, several retina structures such as drusen and macula interfere with the fundus image [8]. Pixels generated by interfering structures and pixels generated within the vessel area have almost identical distribution in terms of intensity.

Recently, some researchers applied deep learning to improve the performance of the accuracy of the edge detection, and achieved good results [9] [10] [11] [12] [13]. These methods take advantages of deep learning to find better feature representations for edges. They aim to build a general model to address the edge detection problems in natural images. Although some of these methods give segmentation results on fundus images [10], these methods based on deep learning mainly work on the edge detection in natural images, which is true that many edge detection problems encountered in

This article has been accepted for publication in a future issue of this journal, but has not been fully edited. Content may change prior to final publication. Citation information: DOI 10.1109/ACCESS.2018.2869858, IEEE Access

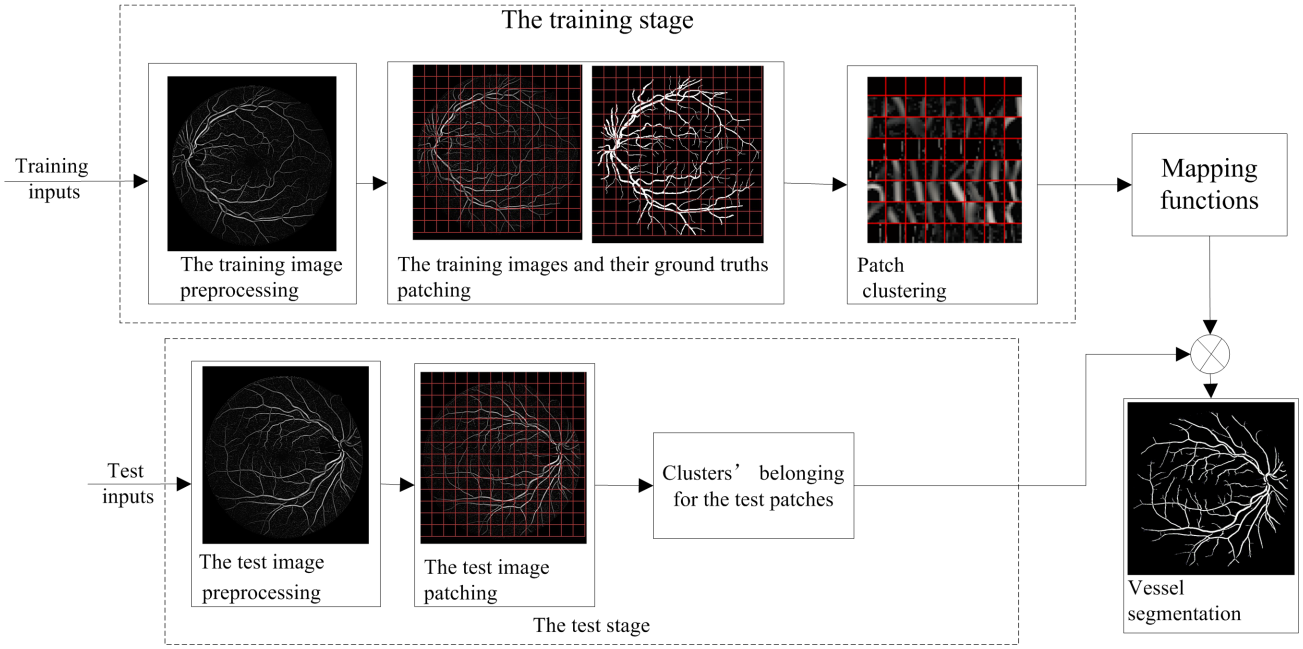

FIGURE 1. The flowchart of the proposed method.

computer vision are almost related to natural images. Compared with fundus images, natural images indeed have more complex structure, but they have less background noise and high contrast relatively. First of all, due to the characteristics of the device, the fundus image is low contrast, which will lead to the degradation of the discriminator's discriminative power. Especially in Super Resolution construction [14] [15] [16]. Learning a priori knowledge without any supervision to effectively represent the main structure of the object. Although clustering in large-scale training data is time consuming, it can be calculated offline and usually only needs to be run once for the application. In the test phase, The computational load is relatively low because this method only needs to determine which cluster the local data belongs to. However, the challenge is how to segment the blood vessels of the fundus image by cluster-based methods. This method has not been explored many times in the literature.

Continuous development of image transform methods has acted as the main motivation for this research. The primary contributions of this paper are threefold. 1) We implement the new classification approach by extending more work on our early stage preliminary work significantly [17]. 2) New results are presented on STARE database, and we give a comparison of our method and six other methods on DRIVE and STARE datasets. 3) The simple and fast mapping functions and processing steps are proposed and validated, this work facilitates the segmentation of the vessel in fundus images. The results show that our method outperforms others on the benchmark DRIVE database and STARE database.

The organization of our paper is as follows. Section 2 provides an overview of classic approaches for the vessel segmentation problem. Section 3 presents the framework of our method in details. The experimental results are given in section 4 and the conclusions are summarized in section 5.

II. RELATED WORK

The unsupervised algorithms have been well recognised in terms of their efficiency of segmenting the vessels in fundus images, such as matched filtering [18], line detectors [19], morphological transformations [20], model-based methods [21], or multiscale vessel segmentation methods [22]. Rangayyan et al. [23] designed a set of Gaussian filters to detect and extract the blood vessels. Miri et al. [24] used multiple structuring elements to extract vessel ridges. Al-Diri et al. [25] improved the traditional active contour model to segment the vessels. Though these algorithms are easily modeled, they are computationally complex.

In contrast, the supervised machine learning has been widely studied in many fields related to image processing. Classic classifiers such as the KNN [26], Gaussian mixture model (GMM) [27], support vector machine (SVM)[22], neural networks [4], and extreme learning machine (ELM) [5] have been applied to distinguish vessel pixels from nonvessel pixels. Staal et al. proposed a ridge-based blood vessel segmentation method in combination with a supervised classification technique [28]. Another SVM-based algorithm, which was also trained on the DRIVE database, was proposed by Ricci and Perfetti [2]. Lupascu et al. [3] proposed an AdaBoost-based classifier to segment the retinal vessels. Fraz et al. used an ensemble system of bagged and boosted decision trees and utilized a feature vector based on the orientation analysis of gradient vector field, morphological transformation,

This article has been accepted for publication in a future issue of this journal, but has not been fully edited. Content may change prior to final publication. Citation information: DOI 10.1109/ACCESS.2018.2869858, IEEE Access

line strength measures, and Gaussian filter responses [29]. Roychowdhury et al. presented a novel three-stage blood vessel segmentation algorithm, which used a Gaussian mixture model (GMM) classifier to combine a set of eight features [30]. Franklin et al. presented a retinal vessel segmentation technique which identified and segmented retinal blood vessels by making use of a multi-layer perception neural network [31].

Finally, structure edge (SE) method proposed by Dollár et al. [32] formulated the problem of predicting local edge masks in a structured learning framework applied to random decision forests. Like in our work, we also attempt to capture local patterns. Instead of computing local edge structures directly from the color image patches, we find the local patterns from the manual segmentation patches. Zhang et al. [12] extended SE method to the field of semi-supervised learning by presenting an effective sparse representation to enable the incorporation of abundant unlabeled patches with their estimated structure labels. Sparse representation is really an effective way to represent local image patches, which has been proven by [33] [34]. We use sparse representation to find a better and compact way to represent the patches in each cluster. In this way, the test patches only need to compute sparse codes among all the dictionaries and choose the one wich has the minimal sparse code error. Ganin et al. [10] proposed a new architecture based on a simple combination of convolutional neural network with the nearest neighbor search. This method bears resemblance to our method on image patch transformation. But our patch transform is more simple and straightforward.

To take the advantages of the unsupervised and the supervised algorithms, we came out with a new method that uses sparse representation and clustering to robustly segment retinal blood vessels. Patch mapping can be seen in many Super-Resolution methods [15] [14] [16]. A large number of patches are randomly extracted from a set of manual segmentation images and clustered into several groups where each group contains a specific local pattern and a mapping function can be learned from corresponding group patch pairs. To reduce the computational complexity, Yang et al. proposed to split the feature space into numerous subspaces and collect exemplars to learn priors for each subspace, thereby creating effective mapping functions [14]. Inspired by Yang et al., We have devised a way to explore the mapping function from the training patch to the corresponding patch by manual segmentation.

III. MAPPING VIA CORRESPONDING PATCH PAIRS

For simplicity and efficient, only the green channel of an color fundus image is used because of its highest contrast among the three channels. Then, Gaussian filters are applied to the green channel with a size of 13*13 Gaussian core and the angle resolution of 15 degrees.

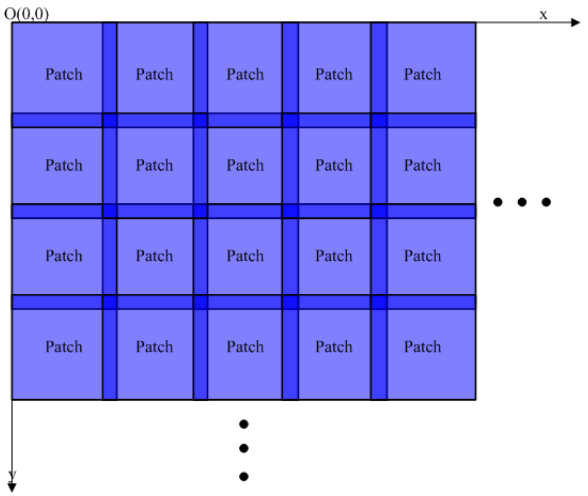

FIGURE 2. Patches overlap (Dark area shows the overlap occurred in each patch).

A. IMAGE PATCHES

Figure 2 shows how to divide the images and their corresponding manual segmentations into a lot of patches. To improve the performance, the image is divided in a way that neighbor patches have limited overlaps. If the patch is set to a proper size, it should contain a simple vessel pattern.

In Figure 2, the point O is the top-left corner of one image. The patches are extracted from the top-left corner to the lower-right corner with a limited overlap.

B. PATCH CLUSTERING

Vessels in a single patch have limited patterns. Therefore, each image can produce a large number of patches. The bigger the patch is, the more patterns it produces. In theory, the number of patterns grows exponentially with the size of the patch. Fortunately, only a small number of the patterns can represent the structure of the whole patches, especially in the case of big patch. Then the question is how to find these representative patterns?

Here, we use a similar method described in [35], which used a data-driven way to capture the edge structures. For the issues of vessel segmentation in fundus image, the focus is the whole vessel segmentation. It has some difference between edge detection and vessel segmentation. The fundus image has a lot of tiny vessels and most of the tiny vessels has only a few pixels wide. Under the noisy background, the tiny vessels are easily regarded as non-edge pixels. So, we choose to find the vessel patterns not just edge structures in patches. To find the vessel patterns, the patches can be clustered under some metric. A easy way is to make use of Euclidean distance by grouping the patches from the manual segmentations.

Referring to clustering, there are many published clustering algorithms. Here, we take the classic K-means clustering algorithm. More details of K-mean can be found in [36]. Figure 3 shows an example of grouping results using 20 training images of size 565 * 584. The number of clusters

This article has been accepted for publication in a future issue of this journal, but has not been fully edited. Content may change prior to final publication. Citation information: DOI 10.1109/ACCESS.2018.2869858, IEEE Access

is set to 256, the size of the patch is set to 10 * 10, and 20 images are used for clustering. Extracted more than 60,000 patches from training images. Each cluster has an average of more than 200 patches. From Figure 3, we can see that the patches in one cluster share the similar pattern as we expect. In the experiment analysis, as we know the largest cluster has more than 500 patches, while the smallest cluster contains less than 100 patches. This is because some shapes in the fundus image appear more often than others. Patches in the same row mean they are selected from the same cluster.

C. PATCH MAPPING FUNCTIONS

One patch in the training image and its corresponding patch in the manual segmentation is named as a pair. Finding the mapping function for the pair, is a major step in vessel segmentation. To find the mapping function, we denote the training patches in cluster i with the matrix M_i, and we denote the corresponding patches from their manual segmentations with the matrix M_{GT_i}, while the mapping function of cluster i is represented by f_i. By mapping function f_i, a relationship between training patches and their corresponding ground truths can be established. The formula is shown below:

$$f_i \times M_i = M_{GT\_i} \tag{1}$$

where f_i is a $k^2 \times k^2$ matrix, M_{GT_i} and M_i have the size of $k^2 \times n_i$, k is patch size, and n_i is the total number of patches in cluster i.

Given that n_i is considerably sizeable than k^2, the result for the mapping function f_i in equation (1) is transformed to get the minimal square result of an over-determined equation where the condition number is good. The final equation can be written as:

$$f_i = M_{GT\_i} \times (M_i)^T \times [M_i \times (M_i)^T]^{-1} \tag{2}$$

Even though the minimal square result is delicate to the outliers. The results of mapping function could be acceptable and it could be determined in the analysis. Therefore error to be solved can be computed using:

$$E_{error} = \sum \| f_i \times M_i - M_{GT_i} \|_2^2 \tag{3}$$

IV. VESSEL SEGMENTATION

Group of clusters with a large number of patches having the same structure are obtained after clustering. To segment vessels in the fundus image, mapping functions of clusters are used. After that, finding the mapping function for each test patch will become the next key question.

In that part, the optimization algorithm of vessel segmentation that based on the nearest centers has been described.

To convert the test image into patches, preprocessing and division described in section 3 are used to a test image. Three measures are important to fragment the vessels for patch and p_{ij} is converted into a vector m_i.

1) Interval D between the cluster centers C and the vector m_i is calculated to know that cluster of the vector m_i with minimum interval d_i for each independent vector. The computation formula is described as:

$$\begin{aligned} d_i &= minD \\ &= min(m_i - c_j) \end{aligned} \tag{4}$$

where $c_j \in C = \{c_1, c_2, \ldots, c_j, \ldots, c_{num}\}$, cluster centers are represented as C, and the number of clusters is num.

2) After getting the cluster center c_j, the mapping function f_j of vector m_i is used to fragment the vessels in the above vector. The fragmentation could be known by the equation (5).

$$m_i^{seg} = f_i \times m_i \tag{5}$$

where m_i^{seg} represents the segmentation result for vector m_i.

3) The vector m_i^{seg} is restored into a patch p_{ij}^{seg}

V. EXPERIMENTAL RESULTS

The performance of our proposed method performance is assessed on both the DRIVE and STARE databases. DRIVE contains a group of 40 images with the size of 565*584, which has been categorised into a training set and a test set equally. For STARE database, it contains 20 images and half of these images are used for training and half are used for test. These experiments were managed in Matlab version 2010a, which has a 3.5GHz Intel Core processor and 4GB of RAM. Here Gaussian filters are used firstly to process the vessel pixels in green channel. In the following experiments, 12 selected angles were used to filter the image.

A. EXPERIMENTAL SETTINGS

Three parameters should be carefully chosen in our performance analysis to achieve better results in the segmentation results. Sensitivity(SE), specificity(SP), accuracy(ACC) has been handpicked as the key performance indicators in this analysis.

$$SE = \frac{TP}{P} = \frac{TP}{TP + FN} \tag{6}$$

$$SP = \frac{TN}{N} = \frac{TN}{TN + FP} \tag{7}$$

$$ACC = \frac{TP + TN}{TP + TN + FP + FN} = \frac{TP + TN}{P + N} \tag{8}$$

where:TP — The number of true vessel pixels segmented;
FP — The number of false vessel pixels segmented;
TN — The number of true background pixels segmented;

This article has been accepted for publication in a future issue of this journal, but has not been fully edited. Content may change prior to final publication. Citation information: DOI 10.1109/ACCESS.2018.2869858, IEEE Access

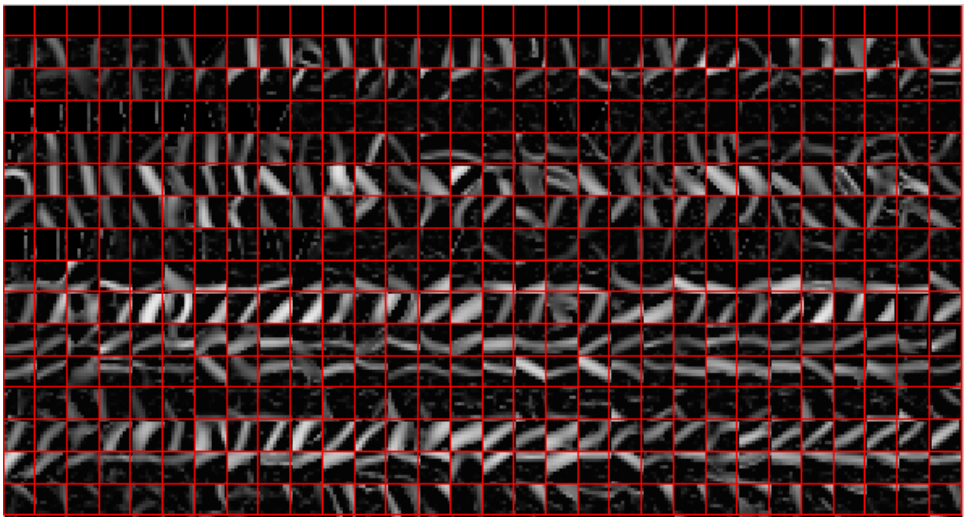

FIGURE 3. 30 patches with size of 10*10 for each clusters selected from 256 clusters.

FN — The number of false background pixels segmented;
P — A total number of vessel pixels in the ground truth;
N — A total number of background pixels in the ground truth.

Patch Size: Structure complexity is directly related to patch Size. The more complex the patch structure is, the larger the patch is. Consequently, the patch size is analyzed to determine the appropriate size for 1*1, 2*2, 3*3, 4*4, 5*5, 7*7, 9*9 and 11*11, where the overlapped pixels are zero pixel, one pixel, two pixels, three pixels and four pixels. The clusters set to 16, 32, 64, 128 and 256 according to the patch size. The performance of our proposed method under various patch sizes are shown in Table 1. The observations shown that, there really has some improvement in SE but no improvement in SP and ACC with the increase of patch size. That is because the bigger the patch size is, the more patterns it contains, so it need more clusters to get satisfactory result. Considering the computing capability of our computer, the patch size is set to 5*5.

Number of Clusters: In this theory, there are 25625 distribution from a patch with size 5*5. The possibility exhaustively exploring are limited due to the memory on a machine with a 4GB RAM. The performance has been analyzed based on different number of clusters, in order to get the relationship between segmentation quality and computational load. The segmentation results of different number of clusters are showed in Column 7 in Table 1. From Column 7 in Table 1, the conclusion of the clusters that we set based on the computer capability will be archived, and the better segmentation could be obtained. Therefore, the 256 clusters have been set that are the highest number we can afford.

From Table 1, we also can conclude that SE and ACC have a positive correlation with the patch size and the number of clusters. As for SP, it shows a positive correlation with the increasing of the patch size and the number of clusters at the beginning. When the patch size and the number of clusters comes to a limit, it gives a negative correlation.

Overlap: Overlapping is a simple and useful method for smoothing joint blood vessels and suppressing noise when the image is converted into patches to be processed, and after treatment these patches are converted to images. Overlap improves the performance of Super Resolution shown in the work of Yang [14]. There are four kinds of overlap with the patch of size 5*5: one pixel, two pixels, three pixels and four pixels. In addition to performance, the changes in the number of patches have been analyzed by us with different overlapping pixels. Table 2 is the analysis of the result done by us. Without overlap, extract 262,160 patches from 20 train images and extract 262,160 patches from the corresponding ground truth. Number of patches for one pixel of overlap is 408900. For two pixels and three pixels overlap, the numbers are 725560 and 1629800 respectively. Four pixels has the largest number of patches that is 6507600. In Table 2, as the number of overlapping pixels increases, we can see that performance is growing steadily. Although the number of patches varies greatly from one size to another, the four pixels have been selected by us to overlap for better segmentation. In our analysis, the results is beyond our expectation that the best performance comes from four pixels overlap. To achieve better vessel segmentation, the enough patches are needed by our method. There are only 20 images have been used to train our model (memory limitation). In order to increasing the overlap pixels, the test image with one pixels may have many outputs. Therefore, the final segmentation that is formed from outputs will be more accurate and robust than the method that without overlap. To some extent, overlap may compensate the loss caused by memory limitations.

B. EXPERIMENTAL EVALUATION AND ANALYSIS

The effect of our method on the segmentation performance is evaluated in two ways: the qualitative analysis and the quantitative analysis. The segmentation performance has

This article has been accepted for publication in a future issue of this journal, but has not been fully edited. Content may change prior to final publication. Citation information: DOI 10.1109/ACCESS.2018.2869858, IEEE Access

TABLE 1. The performance of our method under different patch sizes and different clusters

The number of clusters		1*1	2*2	3*3	4*4	5*5	7*7	9*9	11*11
16	SE	0.7296	0.7419	0.7525	0.7639	0.7641	0.7632	0.7649	0.7665
	SP	0.9668	0.9674	0.9713	0.9728	0.9744	0.9743	0.9738	0.9728
	ACC	0.9431	0.9448	0.9476	0.9502	0.9501	0.9501	0.9499	0.9496
32	SE	0.7383	0.7469	0.7562	0.7637	0.7645	0.7649	0.7650	0.7717
	SP	0.9665	0.9683	0.9728	0.9732	0.9767	0.9745	0.9763	0.9772
	ACC	0.9440	0.9458	0.9487	0.9497	0.9512	0.9511	0.9508	0.9504
64	SE	0.7432	0.7502	0.7623	0.7656	0.7725	0.7729	0.7711	0.7739
	SP	0.9672	0.9712	0.9732	0.9755	0.9783	0.9753	0.9755	0.9746
	ACC	0.9449	0.9473	0.9495	0.9508	0.9528	0.9516	0.9515	0.9513
128	SE	0.7462	0.7638	0.7708	0.7731	0.7743	0.7741	0.7745	0.7744
	SP	0.9682	0.9719	0.9743	0.9762	0.9798	0.9795	0.9790	0.9786
	ACC	0.9456	0.9492	0.9510	0.9530	0.9536	0.9534	0.9533	0.9531
256	SE	0.7464	0.7660	0.7709	0.7733	0.7744	0.7742	0.7746	0.7749
	SP	0.9696	0.9739	0.9779	0.9775	0.9802	0.9804	0.9801	0.9797
	ACC	0.9462	0.9503	0.9524	0.9526	0.9538	0.9538	0.9537	0.9536

TABLE 2. The performance of our method under different overlap

Overlap Pixels	SE	SP	ACC	Number of Patches
0	0.7462	0.9591	0.9408	262160
1	0.7534	0.9644	0.9430	408900
2	0.7595	0.9698	0.9458	725560
3	0.7658	0.9742	0.9483	1629800
4	0.7744	0.9802	0.9538	6507600

been compared to other classical methods, including the Hessian matrix method, the Gaussian filter, and a mixture of Hessian matrix and Gaussian filter. The results of our method and others are showing in Figure 4. The comparative analysis shows that our method is outstanding than others in terms of the segmentation effect. It performs more better in small vessel. Figure 4 shows the zoom details, our method is more fluid and clear, closer to the actual situation.

Table 3 gives the specific segmentation results for our method and the other three methods including the quality analysis and the time cost using the six images in Figure 4. From Table 3, we can know exactly that the segmentation accuracy of our method is better than the other three methods in terms of SE, SP and ACC. In addition, we also can see that the performance of four methods have a big fluctuation in SE and have a relative small fluctuation in SP and ACC. Referring the time cost, our method has two stages: training stage and test stage. Because the training stage can be realized offline, we only consider the test time cost. The combination of Gaussian and Hessian obtains better performance than either Gaussian or Hessian method. Although our method is slower than Hessian matrix method, Gaussian filters method and the mixture of Hessian matrix and Gaussian filters, it is much better than three others in segmentation accuracy.

Table 3 gives the specific segmentation results for our method and the other three methods including the quality analysis and the time cost using the six images in Figure 5. From Table 3, we can know exactly that the segmentation accuracy of our method is better than the other three methods in terms of SE, SP and ACC. In addition, we also can see that the performance of four methods have a big fluctuation in SE and have a relative small fluctuation in SP and ACC. Referring the time cost, our method has two stages: training stage and test stage. Because the training stage can be realized offline, we only consider the test time cost. Although our method is slower than the Hessian matrix method, the Gaussian filter method and the hybrid method of the Hessian matrix and the Gaussian filter, the segmentation accuracy is much better than other methods.

Next, the performance and computational complexity of our approach are shown in Table 4 compared to some typical vessel segmentation methods. Due to time constraints, we are unable to reproduce the segmentation results of typical methods. The results are taken from the work done by Staal et al. [28], Soares et al. [27], Miri et al. [24], Fraz et al. [29], Roychowdhury et al. [30] and Franklin et al. [31]. We tested the segmentation performance of our method and the six typical tasks of the DRIVE database and the STARE database using the same measurement method.

On the DRIVE database, the better segmentations have been achieved by our method in terms of SE and ACC that shown in Table 4. In particular, for SE, our approach improved 8.7 percent for Franklin et al., improved 5.9 percent for Miri et al., improved 5.5 percent improvement for Staal et al., improved 4.9 percent for the GMM-based approach by Roychowdhury et al., improved 4.1 percent for the supervised approach by Soares et al. and improved 3.4 percent for Fraz et al. Significant improvements in SE mean that our approach can divide more of the vascular pixels. With reference to SP, our approach is better than Staal et al., Soares et al. And Miri et al. Our method and the six typical works

This article has been accepted for publication in a future issue of this journal, but has not been fully edited. Content may change prior to final publication. Citation information: DOI 10.1109/ACCESS.2018.2869858, IEEE Access

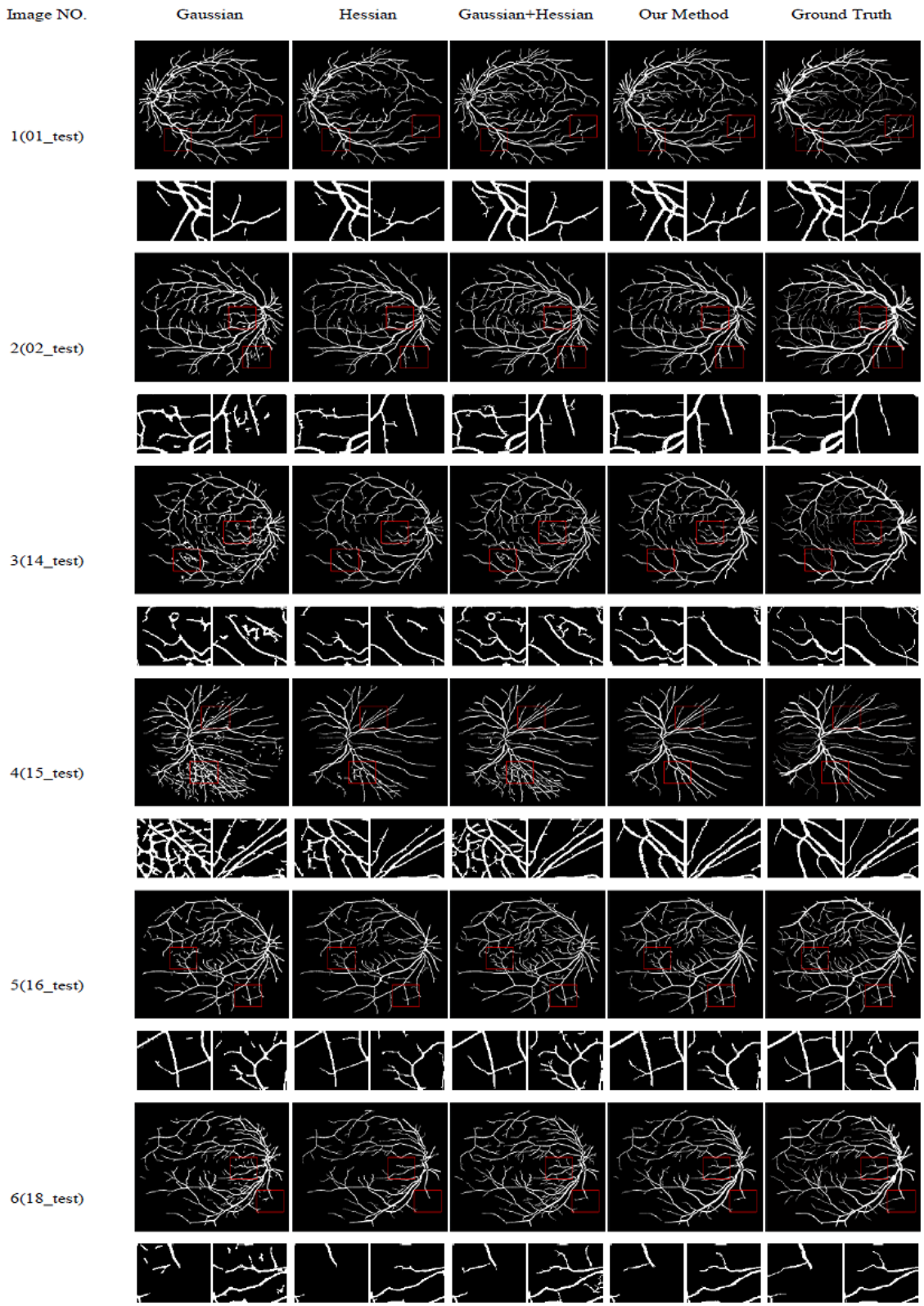

FIGURE 4. Results by our method and the other three methods with adequate zoom level.

This article has been accepted for publication in a future issue of this journal, but has not been fully edited. Content may change prior to final publication. Citation information: DOI 10.1109/ACCESS.2018.2869858, IEEE Access

TABLE 3. Comparison of performance of our method with the other three methods using six images in Figure 4

Image NO.		1	2	3	4	5	6
Gaussian	SE	0.7442	0.6952	0.7029	0.7356	0.7186	0.7464
	SP	0.9772	0.9781	0.9666	0.9564	0.9827	0.9784
	ACC	0.9587	0.9502	0.9467	0.9408	0.9586	0.9609
	Time(s)	8.224	8.753	7.9223	7.6846	7.9398	7.9887
Hessian	SE	0.7595	0.6631	0.6693	0.6615	0.6575	0.6937
	SP	0.9796	0.9866	0.9855	0.9887	0.9901	0.9886
	ACC	0.9587	0.9508	0.9548	0.9553	0.959	0.9613
	Time(s)	15.633	15.562	15.0237	15.2187	14.9173	14.8173
Gaussian+Hessian	SE	0.7809	0.7226	0.7378	0.7472	0.7365	0.7646
	SP	0.979	0.9813	0.9776	0.9737	0.9843	0.98
	ACC	0.9604	0.9548	0.9609	0.9631	0.9612	0.9668
	Time(s)	16.592	17.872	17.0273	16.0228	16.5593	16.4746
Our Method	SE	0.7867	0.7237	0.7534	0.7761	0.7404	0.7771
	SP	0.987	0.9899	0.988	0.9892	0.9933	0.9917
	ACC	0.9637	0.9571	0.9652	0.9678	0.9656	0.9694
	Time(s)	61.97	55.368	54.793	59.519	64.452	62.768

have very small total variance of SP. However, for the one image, the vessel pixels only account for a small part. The great impact on the segmentation performance may be caused by a small variance in SP. Depending on the advantages of SE, our approach is still superior to other methods in the ACC.

On STARE database, we compare our method with four works done by Staal et al., Soares et al., Fraz et al., and Roychowdhury et al.. The performance of our method in ACC is better than the three others except the work done by Fraz et al. Although The performance of our method in SE is better than the performance done by Fraz et al., the performance of our method in SP is lower than the performance done by Fraz et al.. Compared the results of our method on DRIVE database with the results on STARE database, the improvement on DRIVE is much better than the improvement on STARE database. That is because the images in STARE database is more clear and has less abnormity than the images in DRIVE database. So classical methods can also get relatively better results.

VI. CONCLUSIONS

In this paper, we propose a novel approach to robustly segment the retinal blood vessels using the cluster-based patch mapping function and test them on the DRIVE database and the STARE database. The mapping functions can be used as a bridge between color fundus images and its ground conditions. To some extent, our approach is a supervised algorithm that uses a mapping function to learn local patterns from the training data to map the test image to its segmentation. In the experimental analysis, the average time cost is 60 seconds, and our method is superior to the typical method in terms of segmentation accuracy. Thus, it is useful for automated algorithms that detect the density, tortuosity, or width of these peripapillary vessels for severity analysis of pathologies such as vein occlusions and glaucoma. In addition, future work will focus on more standard databases with a variety of related attributes.

ACKNOWLEDGMENT

This work is supported by the National Natural Science Foundation of China (No.61762014; No. 61762018), the Opening Project of Guangxi Colleges and Universities Key Laboratory of robot welding (Guilin University of Aerospace Technology), the Opening Project of Shaanxi Key Laboratory of Complex Control System and Intelligent Information Processing, and the Research Fund of Guangxi Key Lab of Multi-source Information Mining Security (MIMS15-05). This work is also partly supported by the Project of Science and Technology of Jiangxi province (No. 20161BAB202065) and supported by the 2016 Guangxi 100 Youth Talent Program (F-KA16016),and the Colleges and Universities Key Laboratory of Intelligent Integrated Automation, Guilin University of Electronic Technology, China (GXZDSY2016-03), the research fund of Guangxi Key Lab of Multi-source Information Mining & Security (18-A-02-02).

REFERENCES

[1] Michael D Abràmoff, Mona K Garvin, and Milan Sonka. Retinal imaging and image analysis. IEEE reviews in biomedical engineering, 3:169–208, 2010.

[2] Elisa Ricci and Renzo Perfetti. Retinal blood vessel segmentation using line operators and support vector classification. IEEE transactions on medical imaging, 26(10):1357–1365, 2007.

[3] Carmen Alina Lupascu, Domenico Tegolo, and Emanuele Trucco. Fabc: retinal vessel segmentation using adaboost. IEEE Transactions on Information Technology in Biomedicine, 14(5):1267–1274, 2010.

[4] Wilfred Franklin and Edward Rajan. Retinal vessel segmentation employing ann technique by gabor and moment invariants-based features. Applied Soft Computing, 22:94–100, 2014.

[5] Vasanthi Shanmugam and RS D Wahida Banu. Retinal blood vessel segmentation using an extreme learning machine approach. In 2013 IEEE

TABLE 4. Comparative performance of our method with some typical works

Methods	DRIVE			STARE			Time Cost	System Platform
	SE	SP	ACC	SE	SP	ACC		
Staal et al.	0.719	0.977	0.944	0.697	0.981	0.952	15 min	1.0 GHz, 1-GB RAM
Soares et al.	0.733	0.978	0.946	0.720	0.975	0.948	3 min	2.17 GHz, 1-GB RAM
Miri et al.	0.715	0.976	0.943	-	-	-	50s	3 GHz, 1-GB RAM
Fraz et al.	0.74	0.981	0.948	0.755	0.976	0.953	100s	2.27 GHz, 4-GB RAM
Roychowdhury et al.	0.725	0.983	0.952	0.772	0.973	0.951	3s	2.6 GHz, 2-GB RAM
Franklin et al.	0.687	0.982	0.950	-	-	-	-	2.66 GHz,3-GB RAM
Our Method	0.774	0.980	0.954	0.767	–	0.953	60s	3.4 GHz, 4-GB RAM

Point-of-Care Healthcare Technologies (PHT), pages 318–321. IEEE, 2013.

[6] Ana Salazar-Gonzalez, Djibril Kaba, Yongmin Li, and Xiaohui Liu. Segmentation of the blood vessels and optic disk in retinal images. IEEE journal of biomedical and health informatics, 18(6):1874–1886, 2014.

[7] Sohini Roychowdhury, Dara Koozekanani, and Keshab Parhi. Iterative vessel segmentation of fundus images. IEEE Transactions on Biomedical Engineering, 62(7):1738–1749, 2015.

[8] Meindert Niemeijer, Bram Van Ginneken, Michael J Cree, Atsushi Mizutani, Gwénolé Quellec, Clara I Sánchez, Bob Zhang, Roberto Hornero, Mathieu Lamard, Chisako Muramatsu, et al. Retinopathy online challenge: automatic detection of microaneurysms in digital color fundus photographs. IEEE transactions on medical imaging, 29(1):185–195, 2010.

[9] Yu Liu and Michael S Lew. Learning relaxed deep supervision for better edge detection. In Proceedings of the IEEE Conference on Computer Vision and Pattern Recognition, pages 231–240, 2016.

[10] Yaroslav Ganin and Victor Lempitsky. N^ 4-fields: Neural network nearest neighbor fields for image transforms. In Asian Conference on Computer Vision, pages 536–551. Springer, 2014.

[11] Anna Khoreva, Rodrigo Benenson, Mohamed Omran, Matthias Hein, and Bernt Schiele. Weakly supervised object boundaries. arXiv preprint arXiv:1511.07803, 2015.

[12] Zizhao Zhang, Fuyong Xing, Xiaoshuang Shi, and Lin Yang. Semicontour: A semi-supervised learning approach for contour detection. arXiv preprint arXiv:1605.04996, 2016.

[13] Wei Shen, Xinggang Wang, Yan Wang, Xiang Bai, and Zhijiang Zhang. Deepcontour: A deep convolutional feature learned by positive-sharing loss for contour detection. In Proceedings of the IEEE Conference on Computer Vision and Pattern Recognition, pages 3982–3991, 2015.

[14] Chih-Yuan Yang and Ming-Hsuan Yang. Fast direct super-resolution by simple functions. In Proceedings of the IEEE International Conference on Computer Vision, pages 561–568, 2013.

[15] Kwang In Kim and Younghee Kwon. Single-image super-resolution using sparse regression and natural image prior. IEEE Transactions on Pattern Analysis and Machine Intelligence, 32(6):1127–1133, 2010.

[16] Jianchao Yang, John Wright, Thomas Huang, and Yi Ma. Image super-resolution as sparse representation of raw image patches. In Computer Vision and Pattern Recognition, 2008. CVPR 2008. IEEE Conference on, pages 1–8. IEEE, 2008.

[17] Haiying Xia, Shuaifei Deng, Minqi Li, and Frank Jiang. Robust retinal vessel segmentation via clustering-based patch mapping functions. In IEEE International Conference on Bioinformatics and Biomedicine (BIBM), pages 520–523. IEEE, 2016.

[18] AD Hoover, Valentina Kouznetsova, and Michael Goldbaum. Locating blood vessels in retinal images by piecewise threshold probing of a matched filter response. IEEE Transactions on Medical imaging, 19(3):203–210, 2000.

[19] Uyen TV Nguyen, Alauddin Bhuiyan, Laurence AF Park, and Kotagiri Ramamohanarao. An effective retinal blood vessel segmentation method using multi-scale line detection. Pattern recognition, 46(3):703–715, 2013.

[20] Ana Maria Mendonca and Aurelio Campilho. Segmentation of retinal blood vessels by combining the detection of centerlines and morphological reconstruction. IEEE transactions on medical imaging, 25(9):1200–1213, 2006.

[21] Koen A Vermeer, Frans M Vos, HG Lemij, and Albert M Vossepoel. A model based method for retinal blood vessel detection. Computers in Biology and Medicine, 34(3):209–219, 2004.

[22] Attila Budai, Georg Michelson, and Joachim Hornegger. Multiscale blood vessel segmentation in retinal fundus images. In Bildverarbeitung für die Medizin, pages 261–265, 2010.

[23] Rangaraj M Rangayyan, Faraz Oloumi, Foad Oloumi, Peyman Eshghzadeh-Zanjani, and Fabio J Ayres. Detection of blood vessels in the retina using gabor filters. In 2007 Canadian Conference on Electrical and Computer Engineering, pages 717–720. IEEE, 2007.

[24] Mohammad Saleh Miri and Ali Mahloojifar. Retinal image analysis using curvelet transform and multistructure elements morphology by reconstruction. IEEE Transactions on Biomedical Engineering, 58(5):1183–1192, 2011.

[25] Bashir Al-Diri, Andrew Hunter, and David Steel. An active contour model for segmenting and measuring retinal vessels. IEEE Transactions on Medical imaging, 28(9):1488–1497, 2009.

[26] Meindert Niemeijer, Joes Staal, Bram van Ginneken, Marco Loog, and Michael D Abramoff. Comparative study of retinal vessel segmentation methods on a new publicly available database. In Medical Imaging 2004, pages 648–656. International Society for Optics and Photonics, 2004.

[27] João VB Soares, Jorge JG Leandro, Roberto M Cesar, Herbert F Jelinek, and Michael J Cree. Retinal vessel segmentation using the 2-d gabor wavelet and supervised classification. IEEE Transactions on medical Imaging, 25(9):1214–1222, 2006.

[28] Joes Staal, Michael D Abràmoff, Meindert Niemeijer, Max A Viergever, and Bram van Ginneken. Ridge-based vessel segmentation in color images of the retina. IEEE transactions on medical imaging, 23(4):501–509, 2004.

[29] Muhammad Moazam Fraz, Paolo Remagnino, Andreas Hoppe, Bunyarit Uyyanonvara, Alicja R Rudnicka, Christopher G Owen, and Sarah A Barman. An ensemble classification-based approach applied to retinal blood vessel segmentation. IEEE Transactions on Biomedical Engineering, 59(9):2538–2548, 2012.

[30] Sohini Roychowdhury, Dara D Koozekanani, and Keshab K Parhi. Blood vessel segmentation of fundus images by major vessel extraction and subimage classification. IEEE journal of biomedical and health informatics, 19(3):1118–1128, 2015.

[31] S Wilfred Franklin and S Edward Rajan. Computerized screening of diabetic retinopathy employing blood vessel segmentation in retinal images. Biocybernetics and Biomedical Engineering, 34(2):117–124, 2014.

[32] Piotr Dollár and C Lawrence Zitnick. Fast edge detection using structured forests. IEEE transactions on pattern analysis and machine intelligence, 37(8):1558–1570, 2015.

[33] Michael Elad and Michal Aharon. Image denoising via sparse and redundant representations over learned dictionaries. IEEE Transactions on Image processing, 15(12):3736–3745, 2006.

[34] Ren Xiaofeng and Liefeng Bo. Discriminatively trained sparse code gradients for contour detection. In Advances in neural information processing systems, pages 584–592, 2012.

[35] Jayesh H Kotecha and Petar M Djuric. Gaussian particle filtering. IEEE Transactions on signal processing, 51(10):2592–2601, 2003.

[36] John A Hartigan and Manchek A Wong. Algorithm as 136: A k-means clustering algorithm. Journal of the Royal Statistical Society. Series C (Applied Statistics), 28(1):100–108, 1979.

This article has been accepted for publication in a future issue of this journal, but has not been fully edited. Content may change prior to final publication. Citation information: DOI 10.1109/ACCESS.2018.2869858, IEEE Access

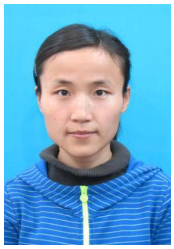

HAIYING XIA received MS and PH.D degrees in the department of electronic and Information engineering from Huazhong University of Science and Technology, Wuhan, China, in 2007 and 2011, respectively. She worked as an associate professor with Guangxi Normal University. Her current research includes pattern recognition, medical image analysis and neural networks.

FRANK JIANG received his Ph.D. degree in the University of Technology Sydney in 2008. He also received the master's degree in computer science and gained the 3.5 years of postdoctoral research experience at the University of New South Wales (UNSW). His main research interests include Data-driven cyber security, Predictive analytics, Biologically inspired learning mechanism and its application in the complex information security system, he has published over 80 high reputated SCI/EI indexed journals and conferences articles.